J. Phys.: Condens. Matter **12** (2000) 2749–2768. Printed in the UK PII: S0953-8984(00)09156-6

S - a - d y b a ya y: a ab y

C Wolverton†, V Ozoliņš‡ and Alex Zunger§

† Ford Research Laboratory, MD3028/SRL, Dearborn, MI 48121-2053, USA
‡ Sandia National Laboratories, Livermore, CA 94551, USA
§ National Renewable Energy Laboratory, Golden, CO 80401, USA

Received 1 November 1999

Ab a . The short-range order (SRO) present in disordered solid solutions is classified according to three characteristic system-dependent energies: (1) formation enthalpies of ordered compounds, (2) enthalpies of mixing of disordered alloys, and (3) the energy of coherent phase separation (the composition-weighted energy of the constituents each constrained to maintain a common lattice constant along an A/B interface). These energies are all compared against a common reference, the energy of incoherent phase separation (the composition-weighted energy of the constituents each at their own equilibrium volumes). Unlike long-range order (LRO), short-range order is determined by energetic competition between phases *at a fixed composition*, and hence only *coherent* phase-separated states are of relevance for SRO. We find five distinct SRO types, and give examples showing each of these five types, including Cu–Au, Al–Mg, GaP–InP, Ni–Au, and Cu–Ag. The SRO is calculated from first principles using the mixed-space cluster expansion approach combined with Monte Carlo simulations. Additionally, we examine the effect of inclusion of coherency strain in the calculation of SRO, and specifically examine the appropriate functional form for accurate SRO calculations.

1. I d : - a d a d a ab y

The equilibrium regions involved in solid-state binary alloy phase diagrams are ordered phases, two-phase regions, and disordered solid solutions. The latter form at elevated temperatures, and consist of an $A_{1-x}B_x$ phase in which the A and B atoms of the alloy are distributed in a disordered fashion on the sites of a single, underlying lattice (often a Bravais lattice, e.g., fcc). In the disordered phase, the atomic-scale occupation of sites of the lattice by A and B atoms does not occur perfectly randomly, nor does it occur with any long-range atomic ordering. Instead, local ordering or local clustering takes place in this solid solution, and is collectively referred to as short-range order (SRO). The degree and type of SRO in a solid solution can be quantified by specifying the Warren–Cowley SRO parameters, α_{lmn}, for a given composition (x) and temperature (T):

$$\alpha_{lmn}(x, T) = 1 - \frac{P_{lmn}^{\mathrm{A(B)}}(x, T)}{x}. \tag{1}$$

Here, $P^{\mathrm{A(B)}}$ $P(x, T)$ is equal to x, and thus $\alpha = 0$. Therefore, the departure of α from zero indicates the extent to which *atom–atom correlations* exist within disordered

incoherent mixtures of phases with different volumes often contain misfit dislocations at the interfaces between the two phases to relieve strain. Thus, the reference energies of equations (3) and (4) involve a state of phase separation (A + B) which is incoherent. Thus, we define the incoherent phase-separated (IPS) state as

$$E_{\mathrm{IPS}} = [(1 - x)E_{\mathrm{A}}(a_{\mathrm{A}}) + xE_{\mathrm{B}}(a_{\mathrm{B}})] \tag{5}$$

and this is simply chosen as the zero reference energy for our comparisons. In contrast, *coherent* two-phase mixtures contain no such misfit dislocations, and thus both phases are somewhat strained due to this constraint of coherency. This leads to:

(c) The coherent phase-separated state or coherency strain (CS), which involves strain in the plane of the interface and relaxation of the atoms perpendicular to the interface. Thus, the strain energy necessary to maintain coherency at an interface between A and B (called the 'coherency strain') is necessarily dependent on the orientation of the interface $\hat{k}$. $E_{\mathrm{CS}}(\hat{k}, x)$, the coherency strain energy, is defined as the energy change when the bulk solids A and B are deformed from their equilibrium cubic lattice constants a_{A} and a_{B} to a common lattice constant $a_{\square}$ in the direction perpendicular to $\hat{k}$, while they are relaxed in the direction parallel to $\hat{k}$†:

$$E_{\mathrm{CS}}(\hat{k}, x) = \min_{a_{\square}} \left[(1 - x) \quad E_{\mathrm{A}}^{\mathrm{epi}}(\hat{k}, a_{\square}) + x \quad E_{\mathrm{B}}^{\mathrm{epi}}(\hat{k}, a_{\square}) \right] \tag{6}$$

where $E_{\mathrm{A}}^{\mathrm{epi}}(\hat{k}, a_{\square})$ is the energy required to deform A biaxially to $a_{\square}$. Each of the energies $E_{\mathrm{A}}^{\mathrm{epi}}$ and $E_{\mathrm{B}}^{\mathrm{epi}}$ is positive definite and, hence, the coherency strain of equation (6) is positive definite. Of particular importance is the lowest attainable coherency strain

$$E_{\mathrm{CS}}^{\mathrm{min}}(x) = \min_{\hat{k}} \quad E_{\mathrm{CS}}(\hat{k}, x) \tag{7}$$

where the minimization is performed over all directions $\hat{k}$. $E_{\mathrm{CS}}^{\mathrm{min}}(x)$ then gives the formation enthalpy of the energetically most favourable coherently phase-separated state.

Using the definitions of equations (3)–(6), we can now note that:

(1) *Long-range order is determined by incoherent phase stability*: for a *long-range-ordered* compound to be a ground state (a zero-temperature stable phase), it must be lower in energy than any other compound at that composition, as well as lower in energy than any *incoherent* two-phase mixture of phases at other compositions, including a mixture of the constituent elements. Thus, a necessary condition for a ground-state structure is that $H_{\mathrm{O}} < 0$. The formation energy H_{O} of equation (3) demonstrates clearly that the long-range order, and hence the equilibrium phase diagram behaviour, is determined by incoherent phase stability.

(2) *Short-range order is determined by coherent phase stability*: the short-range order involves a single-phase field (disordered solid solution) of the phase diagram, and thus does not pertain to incoherent two-phase mixtures. Some of these cases of distinct wavevectors can be explained [8] by noting that whereas SRO is determined by the energetic competition between all possible phases *at a fixed composition*, LRO stability is determined by the energy relative to all possible mixtures of phases, *even those at different compositions*. In fact, two crucial quantities for determining the types of fluctuation which develop in disordered alloys are the 'ordering energy'

$$\delta E_{\mathrm{ord}} = \quad H_{\mathrm{O}} - \quad H_{\mathrm{R}} \tag{8}$$

† In the general case of a low-symmetry (e.g., high-Miller-index) interface, there are three independent plane strain components instead of just the uniform plane strain described by $a_{\square}$ (see reference [22]). Equation (6) is exact for interfaces possessing high-symmetry axes, such as (100) and (111) in fcc-based systems.

and the 'coherent phase-separation energy'

$$\delta E_{\mathrm{CPS}} = E_{\mathrm{CS}}^{\min} - H_{\mathrm{R}}. \tag{9}$$

δE_{ord} (δE_{CPS}) represents the energy required to form the ordered (coherent phase-separated) state, starting from the random alloy of the same composition. Both δE_{ord} and δE_{CPS} are fixed-composition energy differences and are independent of the energy of incoherent phase separation.

Figure 1 illustrates five possible relative orders of the energies H_{O}, H_{R}, and E_{CS} of equations (3)–(6). The ordered structures 'O' in figure 1 are representative of the lowest-energy coherent configurations, i.e., structures with dominant composition waves at the Brillouin zone boundary (e.g., the $L1_0$, $L1_1$, or $L1_2$ structures). It should be noted that in cases (e.g., Al–Cu) where the lowest-energy coherent configurations correspond to ordered compounds which have a large degree of 'clustering', one can obtain clustering-type SRO even in a 'type I' alloy (see reference [12]). In this paper, we study these types I–V of LRO/SRO behaviour in real alloy systems using a first-principles total-energy technique for calculating H_{O} and E_{CS}, and a cluster expansion method for calculating H_{R} and SRO.

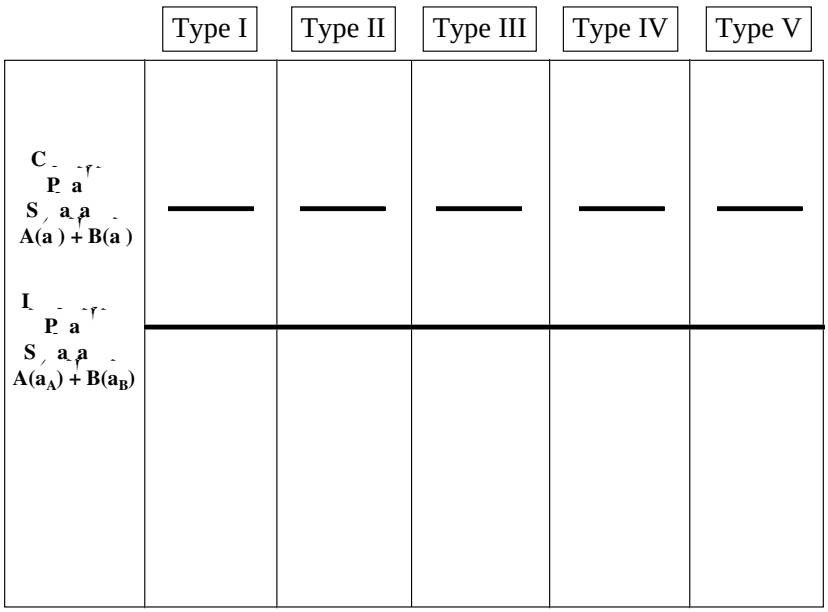

type I: $\delta E_{\mathrm{ord}} < 0 < \delta E_{\mathrm{CPS}}$ (e.g., Cu–Au)
type II: $\delta E_{\mathrm{ord}} < 0 \lesssim \delta E_{\mathrm{CPS}}$ (e.g., Al–Mg)
type III: $\delta E_{\mathrm{ord}} < \delta E_{\mathrm{CPS}} < 0$ (e.g., GaP–InP)
type IV: $\delta E_{\mathrm{ord}} \lesssim \delta E_{\mathrm{CPS}} < 0$ (e.g., Ni–Au)
type V: $\delta E_{\mathrm{CPS}} < \delta E_{\mathrm{ord}} < 0$ (e.g., Cu–Ag).

The arrows in figure 1 show schematically the fluctuations in the random alloy which are energetically most favourable. In 'type I', 'type II', and 'type III' alloys, the ordered alloy is lower in energy than both the random alloy ($\delta E_{\mathrm{ord}} < 0$) and the coherent phase-separated state ($\delta E_{\mathrm{ord}} < \delta E_{\mathrm{CPS}}$). Therefore, energetic fluctuations of the random alloy are expected to be of ordering type, depicted as R $\rightarrow$ O in figure 1. Thus, the SRO of solid solutions of types I, II, and III alloys are all ordering type ($\boldsymbol{k}_{\mathrm{SRO}} \supseteq 0$), even though the LRO is ordering only in types I and II, but phase separating (incoherently) in type III. On the other hand, a 'type V' alloy is a prototypical 'clustering' alloy, where the coherent phase-separated state is lower in energy than both the random alloy ($\delta E_{\mathrm{CPS}} < 0$) and the ordered alloy ($\delta E_{\mathrm{CPS}} < \delta E_{\mathrm{ord}}$). Hence, the SRO is expected to be of clustering type ($\boldsymbol{k}_{\mathrm{SRO}} = 0$), represented by R $\rightarrow$ CS in figure 1. Since phase separation is the lowest-energy incoherent state in a 'type V' alloy, the LRO of this alloy is also phase separation. 'Type IV' alloys are intermediate between 'type III' and 'type V'. In type IV, there is strong competition between ordering and coherent phase separation (δE_{ord}

one assigns the spin-occupation variables, $\hat{S}_i = \pm 1$, to each of the N sites. Within the Ising-like description of the mixed-space CE, the positional degrees of freedom are integrated out, leaving an energy functional of spin variables only, $\hat{S}_i$, which reproduces for each configuration σ the energy of the *atomically relaxed structure*, with atomic positions at their equilibrium (zero-force, zero-stress) values.

The details of construction of this energy functional within the LDA are discussed elsewhere [13, 18], and thus we give here only the salient points. We have used full-potential, fully relaxed, linearized augmented plane-wave method [20] (LAPW) total energies in the construction of the mixed-space cluster expansions. (In the case of GaP–InP, LAPW energies were used to fit a ternary valence-force-field functional, which was in turn used to construct the mixed-space cluster expansion [21].) Details of the LAPW method typically used in these calculations, as well as the number and types of alloy structures used in the CE fit are described in reference [18].

The expression used for the formation enthalpy of any configuration σ in the mixed-space CE is

$$H(\sigma) = \sum_{\boldsymbol{k}} J(\boldsymbol{k})|S(\boldsymbol{k},\sigma)|^2 + \sum_{f} D_f J_f \bar{}_f(\sigma) + \frac{1}{4x(1-x)} \sum_{\boldsymbol{k}} E_{\mathrm{CS}}(\hat{k}, x)|S(\boldsymbol{k},\sigma)|^2. \tag{10}$$

$J($

the cluster expansion of equation (10) *without* E_{CS} and with finite-ranged interactions will give [22] $H(n) \square 1/n$ as $n \rightarrow \infty$, independent of $\hat{k}$. Thus, one must include a E_{CS} term in equation (10) since this introduces the orientation dependence in coherently strained two-phase configurations, which cannot be described by short-ranged real-space interactions $J(R)$. Further, because long-period superlattices possess $\boldsymbol{k} \rightarrow 0$ dominant wavevectors, but the strain energy is dependent on the direction of $\hat{k}$, there is a $\boldsymbol{k} \rightarrow$

disordered alloys as well, i.e., we want to introduce a wavevector dependence into equation (15). Within a second-order expansion of the elastic energy, $\delta E_{\rm rel}$ can be written as [10, 11]

$$\delta E_{\rm rel}(\sigma) = -\sum_{\boldsymbol{k}} V_{\rm rel}(\boldsymbol{k})|S(\boldsymbol{k},\sigma)|^2 \tag{17}$$

where $V_{\rm rel}(\boldsymbol{k})$ can be related to the lattice Fourier transforms of the Kanzaki forces and dynamical matrix [10, 11]. We will retain the form of equation (17), but we will generalize $V_{\rm rel}(\boldsymbol{k})$ to accommodate some of the shortcomings of the second-order expansion derivation.

To gain insight into the wavevector dependence of the relaxation energy, consider the following breakdown of the relaxation energy:

$$\delta E_{\rm rel}(\sigma) = \delta E^{\rm int}_{\rm rel}(\sigma) + \delta E^{\rm ext}_{\rm rel}(\sigma). \tag{18}$$

The cell-internal relaxation $\delta E^{\rm int}_{\rm rel}$ is the energy gained when atomic positions within the unit cell are relaxed, but the unit-cell vectors maintain their ideal angles and lengths, whereas the cell-external relaxation $\delta E^{\rm ext}_{\rm rel}$ is the energy gained when the unit-cell vectors are allowed to relax. For some high-symmetry structures, $\delta E^{\rm int}_{\rm rel} = 0$ by symmetry: structures with dominant composition wavevectors at the Brillouin zone boundary often possess only cell-external degrees of freedom. For example, the A_1B_1 superlattice along (001) is tetragonal, composed of $\boldsymbol{k} = (001)$ waves, and possesses only the tetragonality ratio c/a as a symmetry-allowed degree of freedom. However, the A_2B_2 (001) superlattice is composed of $\boldsymbol{k} = \frac{1}{2}(001)$ waves, and, in addition to the c/a ratio, also possess a cell-internal degree of freedom.

It is interesting to know the extent to which cell-internal and cell-external relaxations are energetically important in various alloy systems. Table 1 shows the LAPW calculated relaxation energy for A_2B_2 and A_1B_1 (001) superlattice structures for a variety of size-mismatched noble-metal and aluminium alloy systems: Ni–Au, Cu–Au, Cu–Ag, Ni–Al, Cu–Al, and Al–Mg. The relaxation energy is decomposed into cell-internal and cell-external pieces. Table 1 demonstrates that (i) when symmetry does not prohibit cell-*internal* relaxation,

Tab 1. LAPW calculated relaxation energies (equation (13)) in a variety of noble-metal and aluminium alloys. Shown are the relaxation energies for A_2B_2 (001) and A_1B_1 (001) superlattices. The former possesses both cell-internal and cell-external degrees of freedom, and the latter possesses only a cell-external degree of freedom. The fraction of the relaxation energy which comes from the cell-internal relaxation is shown, and to give some idea of the scale of the relaxation energy, the ratio between the relaxation energy and the formation enthalpy of the structure is also given.

A_2B_2 (001) superlattice Superlattice	$\delta E_{\rm rel}$	$\delta E^{\rm int}_{\rm rel}/\delta E_{\rm rel}$	$\lvert\delta E_{\rm rel}/H(A_2B_2)\rvert$
Ni_2Au_2	−216.5	0.88	3.08
Cu_2Au_2	−143.1	0.84	21.36
Cu_2Ag_2	−96.7	0.90	1.24
Ni_2Al_2	−303.9	0.50	0.69
Cu_2Al_2	−88.2	0.80	1.19
Al_2Mg_2	−34.6	1.00	2.52
A_1B_1 (001) superlattice Superlattice	$\delta E_{\rm rel}$	$\delta E^{\rm int}_{\rm rel}/\delta E_{\rm rel}$	$\lvert\delta E_{\rm rel}/H(A_1B_1)\rvert$
Ni_1Au_1	−22.0	0.0	0.29
Cu_1Au_1	−12.1	0.0	0.25
Cu_1Ag_1	−7.1	0.0	0.07
Ni_1Al_1	−141.7	0.0	0.21
Cu_1Al_1	−115.9	0.0	0.71
Al_1Mg_1	□ 0	—	□ 0

this mode of relaxation is dominant (e.g., 100% in Al_2Mg_2). Yet, (ii) cell-*external* relaxation is not negligible: it is 100% (by symmetry) for A_1B_1 along (001) or (111); it is □50% for (001) Cu_2Al_2, and □10–15% for Ni_2Au_2 and Cu_2Au_2. (iii) The A_2B_2 structure has much

We next discuss the $F(\boldsymbol{k}) = 1$ form of the coherency strain energy (equation (11)) used in the mixed-space CE of equation (23) and show how it can fail for some short-period superlattices in systems which possess strongly anharmonic strain. The failures include prediction of spurious ground-state structures, and incorrect short-range-order patterns (when compared with measured patterns). Attenuating the form of the coherency strain energy via equation (20) is shown to rectify these problems.

3.3. Attenuating the coherency strain for short-period superlattices

The problems which can arise with the unattenuated form of the CS are most easily explained with an example: Cu-rich Cu–Au alloys. This system has a very large lattice constant mismatch (12%), and thus anharmonic strain effects are significant. First-principles calculations of the coherency strain in Cu–Au alloys [18] have shown that the strong anharmonic strain of Au results in a low CS for the (201) direction in Cu-rich alloys. This simply means that (201) long-period superlattices (small $\boldsymbol{k}$) will be lower in energy than differently oriented long-period superlattices. However, this energetic preference for (201) structures does not necessarily hold for short-period superlattices (large $\boldsymbol{k}$), due to the first two terms of equation (10) which describe interfacial energies of atoms near the Cu/Au interfaces. But the unattenuated form of the coherency strain energy given in equation (11) will give a large energy lowering to *any* Cu-rich structure which possesses composition waves lying along the (210) direction, regardless of the *magnitude* of the wave (the superlattice period). Thus, the short-period Cu_4Au_1 superlattice along (210), which is a structure composperla7ta.5(e)0(o2Ta.5(e)0(o2Ta.5(e)0390.8a5(which)-60(a5(wh

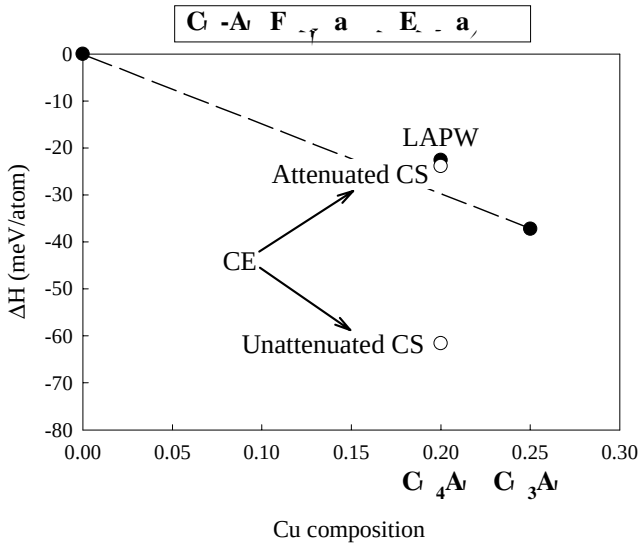

Figure 2. Energetics of the Cu_4Au_1 (210) superlattice relative to Cu_3Au ($L1_2$) and Cu.

(2) The energy of Cu_4Au_1 is brought above the tie line connecting Cu_3Au + Cu; thus, attenuating the CS solves the problem of false ground states due to low-energy long-period strain energies.

(3) Figure 3 shows that the SRO pattern is brought into quantitative agreement with experiment by the attenuation. Calculated peaks in the SRO move from the (210) direction to the (100) direction upon attenuation of the CS.

Thus, we see that the form of the attenuated coherency strain is most likely to be crucial in ordering systems (where wavevectors away from the origin are important) which possess highly anharmonic strain energies (where the soft elastic direction can shift as a function of composition).

Next, we discuss the short-range-order behaviour for a series of alloys classified according to their energetics as in figure 1. We show that the Al–Mg system represents a type II alloy, which has not previously been discussed. We specifically point out the strong effect of attenuating the CS for the Cu–Au and Ni–Au systems, and show that the attenuated strain leads to SRO in Cu-rich Cu–Au alloys in agreement with experiment and significantly changes the predicted SRO in Ni-rich Ni–Au, for which there are currently no measurements.

4. Systematics

We now investigate the SRO/LRO types of figure 1. The calculations for some of these alloy systems (Cu–Au, Ni–Au, and Cu–Ag) have been discussed previously [15] using the unattenuated $F = 1$ form of the coherency strain. Thus, for these alloys, we do not provide a detailed account of the experimental and theoretical literature on the SRO of these solid solutions. Rather, we discuss the effects of attenuating the coherency strain on the SRO, and compare with experimental diffuse scattering measurements where appropriate.

phase is positive, $H_R > 0$, both from experiment [30] and theory [29]. First-principles calculations of the heat of solution of Mg impurities in Al also show a positive formation

the precipitation sequence [29, 32], with this structure being composed of (100) composition waves. The metastable $L1_2$ phase does not appear in the Al–Mg phase diagram because the equilibrium phases are incoherent with the fcc Al matrix; however, in view of the existence of the $L1_2$ phase in coherent precipitation experiments, one might expect the metastable coherent phase diagram to contain this phase. Thus, the (100)-type fluctuations in the SRO are a refl

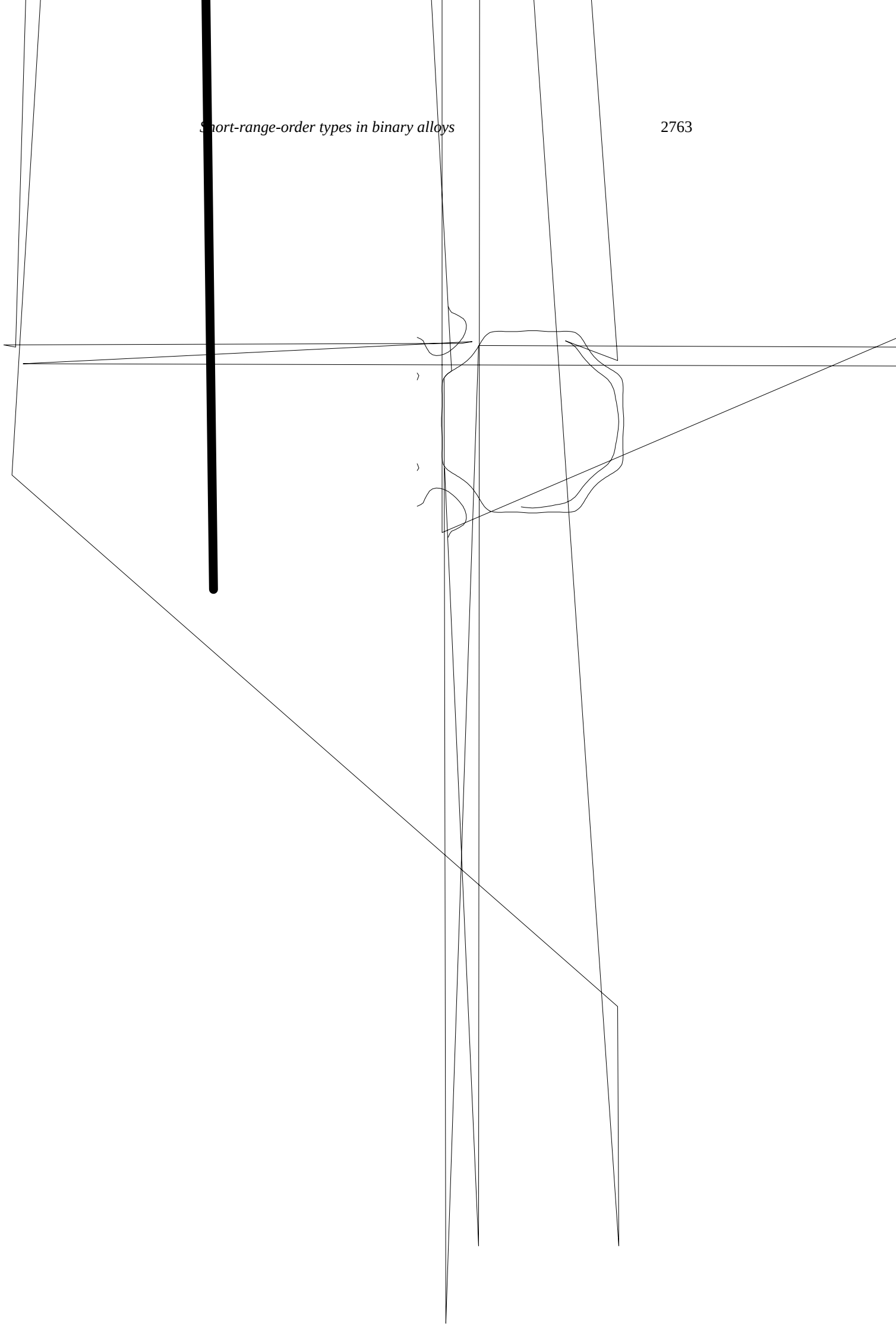

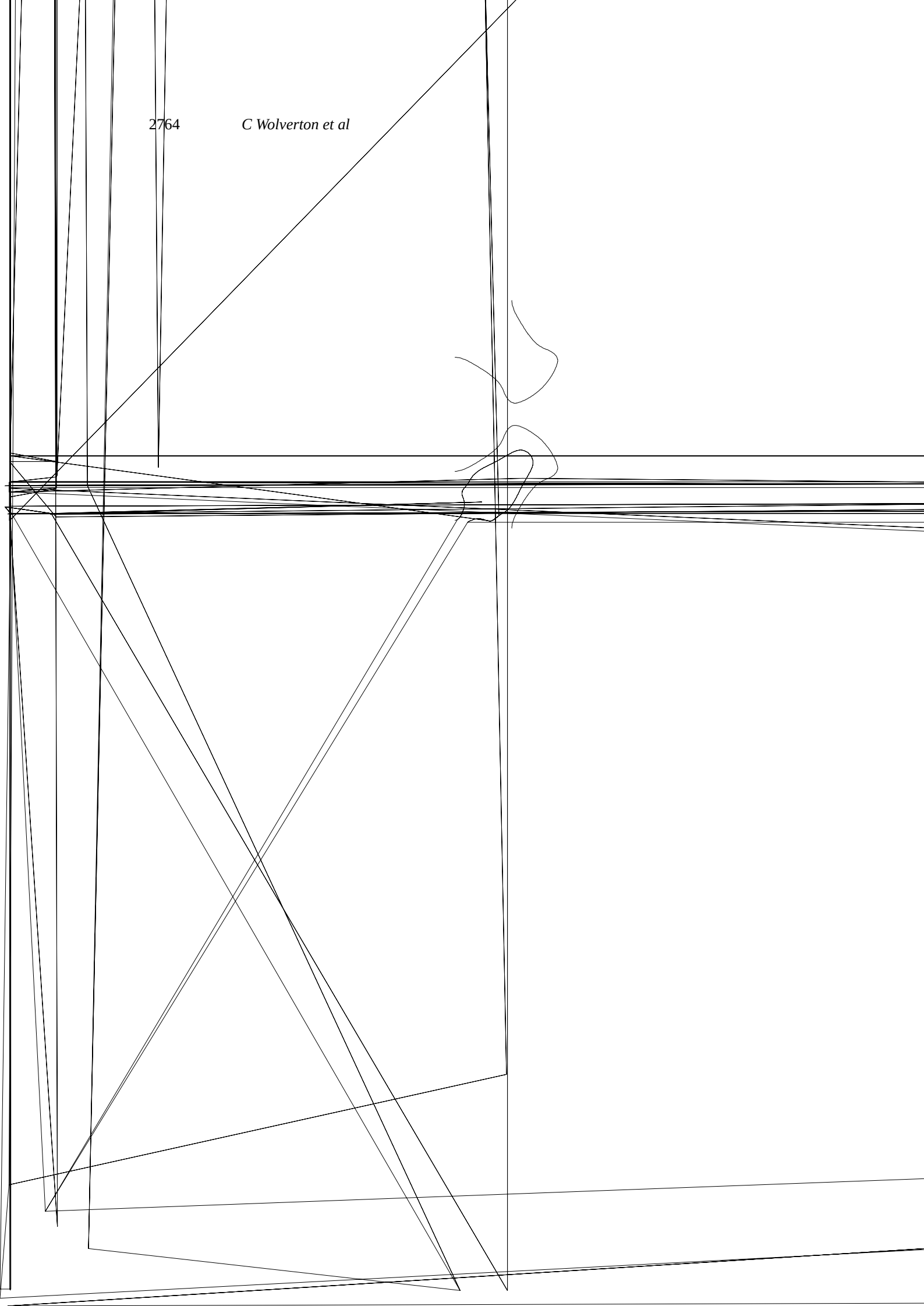

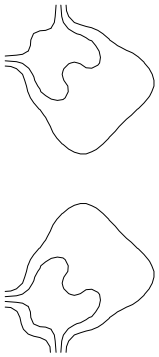

(iii) *Type III (e.g., most semiconductor alloys and perhaps Ti–V)*, where $H_O > 0$ (i.e., phase-separating LRO) and $H_R > 0$ (unstable random alloy), but $H_O < H_R$. Here, the random alloy can lower its energy by adopting ordering-type SRO ($\boldsymbol{k}_{SRO} \neq 0$) even though the LRO is phase separating ($\boldsymbol{k}_{LRO} = 0$). Thus, $\boldsymbol{k}_{LRO} \neq \boldsymbol{k}_{SRO}$.

(iv) *Type IV (e.g., Ni–Au)*, where $H_O > 0$ (i.e., phase-separating LRO) and $H_R > 0$ (i.e., unstable random alloy), but $H_O < H_R$ (as in type III) *and* $E_{CS} < H_R$. Here, the random alloy can lower its energy in *two* channels: by developing fluctuations akin to those of the ordered phase ($\boldsymbol{k}_{SRO} \neq 0$) or fluctuations corresponding to phase separation ($\boldsymbol{k}_{SRO} = 0$).

(v) *Type V (most phase-separating materials, e.g., Cu–Ag)*, where $H_O > 0$ (i.e., phase-separating LRO), $H_R > 0$ (unstable random alloy) *and* $E_{CS} \not< H_O$. Here, the random alloy can lower its energy only by developing phase-separating fluctuations, so both $\boldsymbol{k}_{LRO}$ and $\boldsymbol{k}_{SRO}$ are of clustering type.

This classification scheme (figure 1) enables one to guess the qualitative SRO behaviour of an alloy given the measured or calculated enthalpies of ordered and random systems. It introduces three unusual cases (types II, III, and IV), in addition to the usual ordering (type I) and phase-separating (type V) cases. By noting that SRO reflects a constant-composition energy balance between two phases, one recognizes the possibilities of having ordering SRO coexisting with phase-separating LRO (type III).

To accurately calculate the short-range-order profile we utilize the first-principles mixed-bases cluster expansion (equation (10)), where the coherency strain energy is first separated out from the total energy, and the remainder ('chemical energy') which reflects the constant-composition term is expanded in (a momentum-space series of) pair interactions and in (a real-space series of) many-body interactions. We found here that in those alloy systems where the long-period structures (corresponding to $\boldsymbol{k} \to 0$) have relaxation energies for some ordering directions very different to those of the short-period structures (corresponding to $\boldsymbol{k} \to \pi/n$), a wavevector-dependent term $F(|\boldsymbol{k}|)$ must be introduced into the coherency strain to produce a balanced description. Examples include structures with very large size mismatch such as Cu–Au and Ni–Au, where anharmonic effects lead to large relaxation energies for a particular ordering direction in long-period structures, while short-period structures do not have such a large relaxation. $F(|\boldsymbol{k}|)$ then attenuates the